NIH Public Access
Author Manuscript
Brain Stimul. Author manuscript; available in PMC 2014 April 27.

Published in final edited form as:
Brain Stimul. 2014 ; 7(2): 182–189. doi:10.1016/j.brs.2013.12.013.

Motor Cortex Stimulation Suppresses Cortical Responses to Noxious Hindpaw Stimulation after Spinal Cord Lesion in Rats

Li Jiang[a,c], **Yadong Ji**[a], **Pamela Voulalas**[a,c], **Michael Keaser**[b,c], **Su Xu**[d,e], **Rao P. Gullapalli**[d,e], **Joel Greenspan**[b,c], and **Radi Masri**[a,c,f]

[a]Department of Endodontics, Prosthodontics and Operative Dentistry

[b]Department of Neural and Pain Sciences, University of Maryland School of Dentistry

[c]Program in Neuroscience, University of Maryland School of Medicine Baltimore, Maryland 21201

[d]Department of Sciences of Diagnostic Radiology and Nuclear Medicine, University of Maryland School of Medicine Baltimore, Maryland 21201

[e]Core for Translational Research in Imaging at Maryland (C-TRIM), University of Maryland School of Medicine Baltimore, Maryland 21201

[f]Department of Anatomy and Neurobiology, University of Maryland School of Medicine Baltimore, Maryland 21201

Abstract

Background—Motor cortex stimulation (MCS) is a potentially effective treatment for chronic neuropathic pain. The neural mechanisms underlying the reduction of hyperalgesia and allodynia after MCS are not completely understood.

Objective—To investigate the neural mechanisms responsible for analgesic effects after MCS. We test the hypothesis that MCS attenuates *evoked* blood oxygen-level dependent signals in cortical areas involved in nociceptive processing in an animal model of chronic neuropathic pain.

Methods—We used adult female *Sprague-Dawley* rats (n = 10) that received unilateral electrolytic lesions of the right spinal cord at the level of C6 (SCL animals). In these animals, we performed magnetic resonance imaging (fMRI) experiments to study the analgesic effects of MCS. On the day of fMRI experiment, 14 days after spinal cord lesion, the animals were anesthetized and epidural bipolar platinum electrodes were placed above the left primary motor cortex. Two 10-minute sessions of fMRI were performed before and after a session of MCS (50 μA, 50 Hz, 300 μs, for 30 min.). During each fMRI session, the right hindpaw was electrically stimulated (noxious stimulation: 5 mA, 5 Hz, 3 ms) using a block design of 20 s stimulation off and 20 s stimulation on. A general linear model-based statistical parametric analysis was used to analyze whole brain activation maps. Region of interest (ROI) analysis and paired t-test were used to compare changes in activation before and after MCS in these ROI.

Corresponding Author: Radi Masri, Department of Endodontics, Prosthodontics and Operative Dentistry, University of Maryland Dental School, 650 W Baltimore St. Office #6253, Baltimore, MD 21201, 410-706-8133 (phone), 410-706-1565 (fax), Radi.masriATgmail.com.

Financial Disclosures and Potential Conflicts of Interest: The authors do not have any conflicts of interest.

NIH-PA Author Manuscript
NIH-PA Author Manuscript
NIH-PA Author Manuscript

NIH-PA Author Manuscript

NIH-PA Author Manuscript

NIH-PA Author Manuscript

Results—MCS suppressed evoked blood oxygen dependent signals significantly (Family-wise error corrected $p < 0.05$) and bilaterally in 2 areas heavily implicated in nociceptive processing. These areas consisted of the primary somatosensory cortex and the prefrontal cortex.

Conclusions—These findings suggest that, in animals with SCL, MCS attenuates hypersensitivity by suppressing activity in the primary somatosensory cortex and prefrontal cortex.

Keywords

Functional magnetic resonance imaging (fMRI); neuropathic pain; central pain; motor cortex stimulation; noxious electrical stimulation

Introduction

Central neuropathic pain is defined as pain initiated or caused by lesions or dysfunction in the central nervous system (CNS) (1). The pain is persistent, relentless, debilitating, and difficult to treat (2-4). Motor cortex stimulation (MCS) has emerged as a potential technique for the management of pain in patients who suffer from neuropathic pain (5-12). Both invasive and noninvasive protocols have been proposed for MCS, these include: electrical stimulation with implanted electrodes, repetitive transcranial magnetic stimulation (rTMS) and transcranial direct current stimulation (tDCS) (13-16).

Pain relief occurs progressively after the onset of MCS and persists after the stimulation has ended (17, 18). This intriguing post-stimulation effect can last from minutes to hours and even weeks in some reports (19-23). However, the outcomes of MCS are variable and this modality of treatment is often associated with mixed clinical results. The mixed outcomes are a reflection of the complexity and variability of pain conditions, the lack of well-controlled, randomized clinical trials, and the lack of understanding of the mechanisms underlying MCS-induced analgesia (24, 25).

Neuropathic pain, due to injury of the CNS, commonly manifests as spontaneous, ongoing pain. Therefore, imaging studies in patients with central pain focused on investigating how MCS ameliorates ongoing pain. Using positron emission tomography (PET), researchers demonstrated that analgesia produced after the end of MCS was associated with increased regional cerebral blood flow (rCBF) in the thalamus, anterior cingulate cortex (ACC), prefrontal cortex (PFC), anterior insular cortex (IC), and rostral brainstem. They also found no changes in rCBF in motor areas directly beneath the stimulating electrodes or in the primary somatosensory cortex (S1) (26-28). Based on these findings, it was suggested that MCS attenuates ongoing pain by enhancing the release of endogenous opioids and the activation of the descending inhibitory system (29, 30).

In addition to spontaneous pain, neuropathic pain can also manifest as an increased response to noxious stimuli (hyperalgesia) and as pain in response to previously innocuous stimuli (allodynia) (4, 31, 32). MCS can also attenuate hyperalgesia and allodynia in patients with neuropathic pain (5, 6, 22, 33). However, the neural mechanisms, and cortical structures underlying the reduction of hyperalgesia and allodynia after MCS are not entirely clear. One

NIH-PA Author Manuscript

NIH-PA Author Manuscript

NIH-PA Author Manuscript

functional magnetic resonance imaging study (fMRI) showed that long-term MCS treatment reduces pain evoked by noxious stimuli in patients with post-stroke pain by suppressing activity in the second somatosensory cortex (S2), IC, and PFC (34).

Here, we perform preclinical experiments in rats to further study post-stimulation effects of MCS by assessing changes in regional blood oxygen-level dependent (BOLD) signals in response to noxious stimuli. Specifically, we hypothesize that MCS attenuates *evoked* BOLD signals in cortical areas involved in nociceptive processing in animals with spinal cord lesions.

Methods

This study was carried out in strict accordance with the Animal Welfare Act regulations and Public Health Service guidelines and the International Association for the Study of Pain guidelines. All experimental procedures were approved by the University of Maryland Baltimore, Institutional Animal Care and Use Committee.

Twelve adult female *Sprague-Dawley* rats weighing 260 ± 30 g were used in this study. Two naïve rats were used in initial pilot experiments to optimize and test fMRI and noxious electrical stimulation parameters. The remaining rats (n=10) underwent a surgery to lesion the spinal cord and were used in fMRI experiments to study the effect of MCS on evoked cortical BOLD signals.

Spinal cord lesion (SCL)

To lesion the spinal cord, we used similar procedures to those described previously in (35-37). Briefly, under aseptic conditions, the rats were anesthetized with ketamine/xylazine (80/10 mg/kg, i.p.) and placed on a thermo-regulated heating pad to maintain body temperature. A laminectomy was performed to expose the spinal cord between C5 and T2 and the dura was removed. A quartz-insulated platinum electrode (5 μm tip) was targeted to the anterolateral quadrant in the right side of the spinal cord (1.8 mm lateral to the midline). Direct current (10 μA for 10 sec, repeated 4 times) was delivered through the electrode to produce an electrolytic lesion in the area of C6. After surgery, the muscles and skin were sutured in layers to approximate incision sites. We have shown previously that these unilateral lesions produce ongoing pain and bilateral “below-level” (relative to spinal lesion site) hypersensitivity, and bilateral aberrant activity in the thalamus and cortex (35, 36, 38, 39).

Behavioral testing

Animals were habituated for two weeks prior to behavioral testing. The behavioral tests were conducted on three consecutive days before the SCL surgery (baseline) and at days 7 and 14 after surgery. A dynamic plantar aesthesiometer (Ugo Basile, Comerio, Italy) was used to assess mechanical withdrawal thresholds of the hindpaws as described previously (40). The difference in mechanical withdrawal thresholds at days 7 and 14 from baseline was calculated and divided by baseline thresholds to estimate the percent change in mechanical withdrawal thresholds after SCL. Repeated measures ANOVA on Ranks was

NIH-PA Author Manuscript

NIH-PA Author Manuscript

NIH-PA Author Manuscript

used to test for statistically significant changes in mechanical withdrawal thresholds. A $p<0.05$ was considered significant. Only animals that exhibited significant reduction in hindpaw withdrawal thresholds were included in the study.

FMRI

Animal preparation

On the day of fMRI, 14 days after SCL, the animal was initially anesthetized with isoflurane (2%). The femoral vein contralateral to the spinal lesion was catheterized and connected to an infusion pump (Kent Scientific Corp., MA, USA) to administer α-chloralose anesthesia (an initial i.v. bolus of 60 mg/kg and then at a constant rate of 30 mg/kg/h) for the duration of the experiment (41). Once α-chloralose was administered, isoflurane anesthesia was discontinued.

The animal was attached to a stereotaxic frame and the bone overlying the motor cortex was removed and custom made epidural bipolar platinum electrodes (diameter: 70 μm, exposed tip: 50 μm, distance between the electrodes: 500 μm) were placed above the left primary motor cortex using stereotaxic coordinates (A: −3.6 mm, L: 2.8 mm, D: 7.3 mm relative to Bregma) (18, 39), and stabilized using a thin layer of cyanoacrylate followed by acrylic resin.

In our SCL animals, the lesion disrupts the continuity of the spinothalamic tract and the flow of nociceptive information from the hindpaw contralateral to the lesion to the brain. Therefore, we electrically stimulated the right hindpaw ipsilateral to the lesion site because these animals develop bilateral below level hypersensitivity (18). Two custom-made needle electrodes (160 μm diameter) were inserted under the skin of the right hindpaw, one between digits 1 and 2, and another between digits 3 and 4. These electrodes were later connected to a pre-programed constant current stimulator (ISO-Flex and Master 8, A.M.P.I, Jerusalem) and then secured using surgical tape. Due to the large distance between the stimulation electrodes and the center of the MRI head coils, the stimulation current did not introduce artifacts in the fMRI signal.

After placement of the electrodes, the α-chloralose anesthetized animal was moved to a 7.0 Tesla Bruker Biospin/BioSpec 70/30 USR 30 cm horizontal bore animal MRI scanner (Bruker Biospin MRI GmbH, Germany). The animal was placed in prone position in the Bruker semi cylindrical cradle equipped with warm circulating water channels. The head was carefully secured to a stereotaxic head holder by means of a bite-bar and ear pins to prevent head motion and improve head position consistency through the whole experiments. A Bruker ^{1}H 4-channel animal brain surface coil array was used as the receiver and a Bruker ^{1}H 72 mm linear-volume coil as the transmitter. An MR-compatible small animal monitoring and gating system (SA Instruments, Inc., Stony Brook, New York, USA) was used to continuously monitor the animal body temperature and respiration rate. The animal body temperature was maintained at 36 - 37 °C and respiration rate at 40 - 60 breaths/min.

NIH-PA Author Manuscript

NIH-PA Author Manuscript

NIH-PA Author Manuscript

Acquisition

A three-slice (axial, mid-sagittal, and coronal) scout using fast low angle shot MRI (FLASH) was obtained to localize the rat brain. A fast shimming procedure (FASTMAP) was used to improve the B_0 homogeneity within a region of interest (42). High-resolution T_2-weighted anatomic MRI images in coronal direction were obtained by using a rapid 2D acquisition with the relaxation enhancement (RARE) sequence. The parameters were repetition time TR = 4500 ms; echo time TE = 28 ms; number of average = 2; slice thickness = 1 mm; slice gap = 0.1 mm; in-plane spatial resolution of 0.1 mm × 0.1 mm; image matrix size of 256 × 256, and filed of view (FOV) of 2.56 cm × 2.56 cm.

Following the anatomic images, two 10-minute fMRI sessions were performed while the right hindpaw was electrically stimulated. A square wave current with amplitude of 5 mA, frequency of 5 Hz, and pulse duration of 3 ms was used for noxious electrical hindpaw stimulation. The hindpaw was stimulated using a block design with interleaved trials of stimulation off (20 s) and stimulation on (20 s) for a total duration of 10 minutes. In between imaging sessions, MCS electrodes were connected to an isolated pulse stimulator (A-M systems, Sequim, WA, USA) and the motor cortex was stimulated for 30 minutes (square wave pulses with intensity of 50 μA, frequency of 50 Hz, and duration of 300 μs). These parameters have been shown to significantly reduce mechanical hypersensitivity with effects lasting for approximately 90 minutes after stimulation in animals with SCL (18). After MCS, the stimulating electrodes were disconnected from the stimulator. Figure 1 details the experimental protocol.

In each fMRI session, identical anatomical geometry and single shot echo planar imaging (EPI) sequence were used to obtain the fMRI scans. The fMRI parameters used were: repetition time TR = 1000 ms; echo time TE = 27.466 ms; number of average = 1; slice thickness = 1 mm; slice gap = 0.1 mm; in-plane spatial resolution of 0.4 mm × 0.4 mm; image matrix size of 64 × 64, and field of view (FOV) of 2.56 cm × 2.56 cm. Using this sequence, 20 contiguous and interleaved coronal slices were obtained which covered almost the whole brain. The total acquisition time was 10 minutes and there were a total of 600 brain volumes for each fMRI session.

Pilot study in naïve animals

Before performing the experiment in SCL animals, we investigated if our electrical stimulation protocol (20 sec stimulation off and 20 sec stimulation on for 10 minutes), of the hindpaw, elicits somatotpically specific and reliable BOLD responses in naïve animals. Figure 2A shows that left hindpaw stimulation evokes reliable BOLD responses in the hindlimb representation area of the right S1 whereas Figure 2B shows that right hindpaw stimulation in the same animal evokes BOLD response in the left S1.

Data analysis

Analysis of the fMRI time series was performed using MATLAB software (Mathworks, Natick, MA) and SPM 8 software (http://www.fil.ion.ucl.ac.uk/spm/). Prior to statistical analysis, a series of preprocessing procedures were performed: slice timing correction,

NIH-PA Author Manuscript

NIH-PA Author Manuscript

NIH-PA Author Manuscript

realignment, co-registration, and normalization. The slice-timing correction was used to ensure the image data on each slice correspond to the same time point and thus to increase the robustness of the fMRI data analysis (43). A least-square approach and a six-parameter rigid body spatial transformation (44) were used to realign all the time series images of fMRI to the reference time point images in order to remove motion-related artifacts. The obtained movement parameters were used later as part of the regression factors for BOLD signal analysis. The averaged fMRI images were co-registered to the anatomic images of each rat. All the fMRI images were normalized to a reference template. The reference template was obtained as an average of the well-registered high-resolution T2-weighted anatomical images obtained from the SCL animals. High-pass time series filter (> 0.008Hz) and a standard isotropic Gaussian spatial smoothing filter with kernel of FWHM of 0.8 mm were applied to the normalized brain volumes to increase the signal-to-noise ratio and improve the activation detectability.

A general linear model (GLM)-based statistical parametric analysis was employed to assess the activation maps. The BOLD response to hindpaw stimulation was modeled with block design function convolved with a canonical hemodynamic response function (HRF) with motion parameters. For each animal, a first level model with two fMRI sessions were used to obtain t-contrast maps for before MCS, after MCS, and difference between the two sessions. In each session, motion artifacts were corrected using motion parameters obtained from the corresponding session. Regions of interest (ROIs) (45) were defined to further investigate the effect of MCS on specific cortical structures shown previously to be activated in SCL and during MCS. These *a priori* selected areas include the prefrontal cortex (PFC), anterior cingulate cortex (ACC), primary somatosensory cortex (SI), second somatosensory cortex (S2), insular cortex (IC), thalamus, and periaqueductal grey (PAG). All the ROIs were delineated with AFNI ROI drawing tool (46) on the structural T2-weighted images with reference to the Paxinos and Watson rat brain atlas (47). Small volume corrections using Gaussian random field theory (48) was used for the voxel-wise analysis and multiple comparison control restricted to the ROIs. The thresholds of $p = 0.05$ (family-wise corrected) and minimum cluster size of 5 contiguous voxels was applied to obtain the activated voxels within each ROI. Group analysis was performed using the paired t-test on the statistical results of each ROI of individual rats.

Results

Ten animals received lesions in the right anterior quadrant of the spinal cord at C6. In these animals, behavioral tests were performed on both hindpaws at three consecutive days before SCL and at days 7 and 14 post-lesion. Animals with SCL exhibited significant bilateral reduction in mechanical withdrawal thresholds at days 7 and 14 after SCL as shown in Figure 3. Contralateral to the lesion site (left hindpaw), mechanical withdrawal thresholds were reduced by 42.8 ± 6.8% (Mean ± SE) at day 7 and by 43 ± 7.8% at day 14 ($p < 0.001$). Similar findings were observed for the right hindpaw and mechanical withdrawal thresholds were reduced by 36 ± 7.8% at day 7 and 36 ± 7.6% at day 14 ($p < 0.001$). These results are consistent with our previous studies demonstrating that animals with SCL develop bilateral reduction in mechanical withdrawal thresholds and below-level hypersensitivity (31, 36, 38, 39).

NIH-PA Author Manuscript

NIH-PA Author Manuscript

NIH-PA Author Manuscript

In the same animals (n=10) 14 days after SCL, FMRI scans were performed before and after MCS. In Figure 4A, activation maps of a representative example of one animal with SCL are shown. In this animal, electrical stimulation of the hindpaw (before MCS) resulted in significant activation in PFC, ACC, S1, and S2 bilaterally. This bilateral activation is in stark difference from data obtained from naïve animals (Fig. 2 and (49)) and consistent with previous studies demonstrating that spinal cord injury is associated with the expansion of activated areas in cortical regions involved in nociceptive processing (50-52).

We have shown previously that hypersensitivity and ongoing pain are significantly attenuated in animals with SCL after MCS (50 μA, 50 Hz, 300 μs, for 30 min) (18, 39). We also found that these post-stimulation effects last for approximately 90 minutes after the end of stimulation (18). Therefore, in the same animal (Figs. 4A and 4B), we stimulated the MCS for 30 minutes and acquired another fMRI scan. In this example, BOLD signals evoked by electrical hindpaw stimulation were markedly reduced compared to pre-stimulation (Fig. 4B). To compare the difference in area activated before and after MCS, a first level model within SPM was designed and two T contrasts were defined to assess the increased and decreased activation in clusters after MCS (see Methods). Figure 4C depicts both the increased (red) and decreased BOLD signal (blue) clusters in the same animal shown in 4A and 4B. After MCS, a significant reduction in BOLD signals in response to noxious hindpaw stimulation was observed bilaterally in S1, S2, and PFC. Only a small region within the right thalamus exhibited increased activation. Results from 3 animals were excluded from statistical analysis because head position in 2 animals changed due to improper fixation and in one animal, electrical stimulation of the hindpaw failed to evoke BOLD responses.

Next, we performed ROI-based small volume analysis in each animal to assess changes in activation maps in S1, S2, PFC, ACC, IC, Thalamus, and PAG (Fig. 5A). Figure 5B and Figure 5C show the group results of the extracted cluster volume within the activated areas of S1 and PFC bilaterally. There was a significant reduction in cluster volume in the PFC ($p<0.02$) and S1 ($p<0.05$) (Fig. 5B, Table 1). There was no significant change in all other ROIs including S2, thalamus, and PAG. The reduction in BOLD signals in the PFC and S1 after MCS is in line with the long-term effects of MCS observed in clinical studies (34).

Discussion

Our overarching hypothesis is that MCS reduces evoked BOLD signals in cortical structures involved in pain processing. We performed fMRI experiments on an animal model of hypersensitivity after SCL to investigate post-stimulation effects of MCS on evoked cortical BOLD signals. Our results demonstrate that after MCS, evoked BOLD signals are significantly attenuated in S1 and PFC, two structures heavily implicated in nociceptive processing.

MCS suppresses BOLD responses in S1 and PFC

The role of S1 in pain processing, especially the sensory discriminative aspects of pain, is well established (53-57). It is also well established that neuropathic pain following SCL or

NIH-PA Author Manuscript

NIH-PA Author Manuscript

NIH-PA Author Manuscript

injury is associated with deafferentation, thalamocortical asynchrony, and increased afferent drive in S1 in both animals (37, 38, 58, 59) and humans (60-63). Therefore, suppressed evoked BOLD signals in S1 could explain the increase in mechanical withdrawal thresholds, or reduced hypersensitivity, observed in animals after MCS (18, 39).

Previous studies investigating brain activation using PET showed no significant changes in S1 after MCS (17, 28). These studies assessed the effect of MCS on ongoing pain and no noxious stimulation was performed. Clinical studies that used noxious stimuli to study the effect of MCS found that MCS attenuated BOLD signals in the somatosensory cortex (34) which is consistent with our findings.

The PFC is implicated in higher cognitive and emotional functions (64) and is part of pain networks involved in the processing of the affective emotional aspects of pain (65-67). Therefore, the reduced activity in PFC and S1 after MCS suggests that MCS affects both, the sensory discriminative and affective emotional aspects of pain processing.

MCS produced bilateral reduction in evoked BOLD responses in S1 and PFC. This is consistent with several neuroimaging studies showing that MCS effects can be bilateral and can induce changes in activity in remote cortical and subcortical areas (30, 68-72). The bilateral effect of MCS is also consistent with results from animal studies showing that MCS produces bilateral reduction in behavioral metrics of pain. (18, 73). This bilateral effect may result from the transcallosal activation of the contralateral motor cortex (74-76) or through the activation of interhemispheric connections between motor cortices (77, 78).

In this project, the animals were anesthetized during fMRI scans and MCS. Therefore, we were not able to directly test the relationship between the reduction in mechanical thresholds after MCS (18, 39) and changes in stimulus-evoked BOLD responses in S1 and PFC. Anesthesia is known to depress metabolic activity, reduce basal blood flow (41, 79), and diminish BOLD signals and disrupt cortical networks (80, 81). In future experiments, it will be useful to correlate changes of behavioral metrics of pain with changes in brain activation maps produced by MCS in awake animals.

Mechanisms of MCS-induced analgesia

The reduced activity in S1 and PFC after MCS could be due to the activation of the endogenous opioid system (17, 29). Indeed, it has been shown that long-term MCS (7 months) changes the availability of opioid receptors in ACC, PAG, PFC, and cerebellum (29). The activation of the descending inhibitory system suppresses nociceptive ascending inputs to the thalamus and the cortex and may result in analgesia. Consistent with this notion, animal studies reported that MCS disinhibits the activity of neurons in the PAG (82-84). However, the majority of these studies were performed in naïve animals, not in animals suffering from chronic neuropathic pain. Further, these animal studies were only limited to studying acute changes in neuronal activity, at a very short temporal scale during MCS, and did not assess post MCS effects.

Another mechanism, by which MCS can reduce activity in S1 and PFC, is through the activation of inhibitory inputs within the thalamus (36, 39, 40). The motor cortex projects

NIH-PA Author Manuscript

NIH-PA Author Manuscript

NIH-PA Author Manuscript

heavily upon the GABAergic nucleus zona incerta a nucleus known to regulate the flow of somatosensory and nociceptive information in the thalamus (36, 40). In animals with central neuropathic pain, activity in zona incerta is abnormally reduced resulting in enhanced activity in the posterior and mediodorsal thalamus (36, 40) and S1 (37). MCS enhances activity in the zona incerta and attenuates activity in the posterior thalamus (40) and reversible inactivation of zona incerta blocks the analgesic effects of MCS (18). These findings suggest that zona incerta plays a role in mediating the analgesic effects of MCS and that reduced BOLD responses in S1 after MCS could be due to the activation of the incertothalamic circuitry.

Similarly, the PFC has strong reciprocal connections with the mediodorsal thalamus, which exhibit a significant increase in neuronal activity in animals with SCL (85). The mediodorsal thalamus is also regulated by inputs from the zona incerta (86) and MCS may attenuate activity in the mediodorsal thalamus and its connections to the PFC by activating the zona incerta (85).

Methodological considerations

A major concern when using electrical stimulation to evoke cortical responses is whether or not these stimuli are noxious. To allay this concern, we used electrical stimulation parameters that preferentially activate nociceptors. We used a stimulus (5.0 mA) that is approximately 5 times higher than the minimum amplitude necessary to elicit a noxious response in awake animals (87). We also used a frequency of 5 Hz that preferentially activates nociceptors (C and Aδ fibers) (88, 89). We also chose a relatively long pulse width (3 ms) because a pulse width of more than 1 ms is recommended in fMRI studies to induce strong and reliable activation of brain structures (90-96).

In addition, we used a surface coil to measure evoked BOLD responses. Therefore, the coil is more sensitive to changes in superficial brain structures rather than the deep structures such as the thalamus and PAG. This could be an additional reason why we did not find significant activation in these areas after hindpaw stimulation.

Another potential concern is the susceptibility artifacts introduced by the electrodes in the motor cortex. Although platinum electrodes are biocompatible (97, 98) and MRI-compatible (99), due to a large discontinuity of magnetic properties around the electrode, susceptibility artifacts (e.g., signal loss, image blurring, geometric distortion) in fMRI images might be significant (100). Our experiments carefully minimized this risk by placing the electrodes between the skull and the dura and by using very fine electrodes with diameter of 70 μm and exposed tip of 50 μm. These electrodes produced negligible susceptibility artifacts and did not affect our analysis of BOLD response in individual animal.

Acknowledgments

We would like to acknowledge Dr. David Seminowicz and Dr. Yihong Yang for their assistance in analyzing fMRI results.

This project was supported by the National Institute of Neurological Disorders and Stroke Research Grant R01-NS069568 and the Department of Defense Research Grant SC090126 to R.M.

NIH-PA Author Manuscript

NIH-PA Author Manuscript

NIH-PA Author Manuscript

References

1. Merskey, H.; bogduk, N. Classification of chronic pain. IASP press; 1994.
2. Baastrup C, Finnerup NB. Pharmacological management of neuropathic pain following spinal cord injury. CNS Drugs. 2008; 22:455–75. [PubMed: 18484790]
3. Siddall PJ, Loeser JD. Pain following spinal cord injury. Spinal Cord. 2001; 39:63–73. [PubMed: 11402361]
4. Finnerup NB, Baastrup C. Spinal cord injury pain: mechanisms and management. Curr Pain Headache Rep. 2012; 16:207–16. [PubMed: 22392531]
5. Tsubokawa T, K Y, Yamamoto T, Hirayama T, Koyama S. Chronic motor cortex stimulation for the treatment of central pain. Acta Neurochir Suppl (Wien). 1991; 52:137–9. [PubMed: 1792954]
6. Lima MC, Fregni F. Motor cortex stimulation for chronic pain: systematic review and meta-analysis of the literature. Neurology. 2008; 70:2329–37. [PubMed: 18541887]
7. Previnaire JG, Nguyen JP, Perrouin-Verbe B, Fattal C. Chronic neuropathic pain in spinal cord injury: efficiency of deep brain and motor cortex stimulation therapies for neuropathic pain in spinal cord injury patients. Ann Phys Rehabil Med. 2009; 52:188–93. [PubMed: 19909709]
8. Velasco F, Arguelles C, Carrillo-Ruiz JD, Castro G, Velasco AL, Jimenez F, et al. Efficacy of motor cortex stimulation in the treatment of neuropathic pain: a randomized double-blind trial. J Neurosurg. 2008; 108:698–706. [PubMed: 18377249]
9. Tsubokawa T, K Y, Yamamoto T, Hirayama T, Koyama S. Treatment of thalamic pain by chronic motor cortex stimulation. Pacing Clin Electrophysiol. 1991; 14:131–4. [PubMed: 1705329]
10. Brown JA, Barbaro NM. Motor cortex stimulation for central and neuropathic pain: current status. Pain. 2003; 104:431–5. [PubMed: 12927615]
11. Osenbach RK. Motor cortex stimulation for intractable pain. Neurosurg Focus. 2006; 21:E7. [PubMed: 17341051]
12. Saitoh Y, Y T. Stimulation of primary motor cortex for intractable deafferentation pain. Acta Neurochir Suppl. 2007; 97:51–6. [PubMed: 17691289]
13. Nguyen JP, Nizard J, Keravel Y, Lefaucheur JP. Invasive brain stimulation for the treatment of neuropathic pain. Nat Rev Neurol. 2011; 7:699–709. [PubMed: 21931348]
14. Nizard J, Raoul S, Nguyen JP, Lefaucheur JP. Invasive stimulation therapies for the treatment of refractory pain. Discov Med. 2012; 14:237–46. [PubMed: 23114579]
15. Nizard J, Lefaucheur JP, Helbert M, de Chauvigny E, Nguyen JP. Non-invasive stimulation therapies for the treatment of refractory pain. Discov Med. 2012; 14:21–31. [PubMed: 22846200]
16. Brown JA. Motor cortex stimulation. Neurosurg Focus. 2001; 11:E5. [PubMed: 16519425]
17. Garcia-Larrea L, Peyron R. Motor cortex stimulation for neuropathic pain: From phenomenology to mechanisms. Neuroimage. 2007; 37:S71–9. Review. [PubMed: 17644413]
18. Lucas JM, Ji Y, Masri R. Motor cortex stimulation reduces hyperalgesia in an animal model of central pain. Pain. 2011; 152:1398–407. [PubMed: 21396776]
19. Khedr EM, Ahmed MA, Fathy N, Rothwell JC. Therapeutic trial of repetitive transcranial magnetic stimulation after acute ischemic stroke. Neurology. 2005; 65(3):466–8. [PubMed: 16087918]
20. Lefaucheur JP, Drouot X, Menard-Lefaucheur I, Nguyen JP. Neuropathic pain controlled for more than a year by monthly sessions of repetitive transcranial magnetic stimulation of the motor cortex. Neurophysiol Clin. 2004; 34:91–5. [PubMed: 15130555]
21. Mertens P, Nuti C, Sindou M, Guenot M, Peyron R, Garcia-Larrea L, et al. Precentral cortex stimulation for the treatment of central neuropathic pain: results of a prospective study in a 20-patient series. Stereotact Funct Neurosurg. 1999; 73:122–5. [PubMed: 10853116]
22. Tsubokawa T, Katayama Y, Yamamoto T, Hirayama T, Koyama S. Chronic motor cortex stimulation in patients with thalamic pain. J Neurosurg. 1993; 78:393–401. [PubMed: 8433140]
23. Jiang, L.; Cha, M.; Ji, Y.; Masri, R. A longitudinal electrophysiological and behavior study on mechanism of pain relief following motor cortex stimulation in an animal model of spinal cord injury pain. Society for Neuroscience; New Orlean, LA: 2012.

NIH-PA Author Manuscript

NIH-PA Author Manuscript

NIH-PA Author Manuscript

24. Cruccu G, Aziz TZ, Garcia-Larrea L, Hansson P, Jensen TS, Lefaucheur JP, et al. EFNS guidelines on neurostimulation therapy for neuropathic pain. Eur J Neurol. 2007; 14:952–70. [PubMed: 17718686]
25. O'Connell NE, Wand BM. Repetitive transcranial magnetic stimulation for chronic pain: time to evolve from exploration to confirmation? Pain. 2011; 152:2451–2. [PubMed: 21703764]
26. Garcia-Larrea L, Peyron R, Mertens P, Gregoire MC, Lavenne F, Le Bars D, et al. Electrical stimulation of motor cortex for pain control: a combined PET-scan and electrophysiological study. Pain. 1999; 83:259–73. [PubMed: 10534598]
27. Garcia-Larrea L, Peyron R, Mertens P, Laurent B, Mauguiere F, Sindou M. Functional imaging and neurophysiological assessment of spinal and brain therapeutic modulation in humans. Arch Med Res. 2000; 31:248–57. [PubMed: 11036174]
28. Peyron R, Garcia-Larrea L, Deiber MP, Cinotti L, Convers P, Sindou M, et al. Electrical stimulation of precentral cortical area in the treatment of central pain: electrophysiological and PET study. Pain. 1995; 62:275–86. [PubMed: 8657427]
29. Maarrawi J, Peyron R, Mertens P, Costes N, Magnin M, Sindou M, et al. Motor cortex stimulation for pain control induces changes in the endogenous opioid system. Neurology. 2007; 69:827–34. [PubMed: 17724284]
30. Peyron R, Laurent B, Garcia-Larrea L. Functional imaging of brain responses to pain. A review and meta-analysis (2000). Neurophysiol Clin. 2000; 30:263–88. [PubMed: 11126640]
31. Masri, R.; Keller, A. Chronic pain following spinal cord injury. In: Jandial, R.; Chen, MY., editors. Regenerative biology of the spine and spinal cord. Austin: Landes Biosciences; 2012. p. 74-85.
32. Greenspan JD, Ohara S, Sarlani E, Lenz FA. Allodynia in patients with post-stroke central pain (CPSP) studied by statistical quantitative sensory testing within individuals. Pain. 2004; 109:357–66. [PubMed: 15157697]
33. Fontaine D, Hamani C, Lozano A. Efficacy and safety of motor cortex stimulation for chronic neuropathic pain: critical review of the literature. J Neurosurg. 2009; 110:251–6. [PubMed: 18991496]
34. Ohn SH, Chang WH, Park CH, Kim ST, Lee JI, Pascual-Leone A, et al. Neural correlates of the antinociceptive effects of repetitive transcranial magnetic stimulation on central pain after stroke. Neurorehabil Neural Repair. 2012; 26:344–52. [PubMed: 21980153]
35. Wang G, Thompson SM. Maladaptive homeostatic plasticity in a rodent model of central pain syndrome: thalamic hyperexcitability after spinothalamic tract lesions. J Neurosci. 2008; 28:11959–69. [PubMed: 19005061]
36. Masri R, Quiton RL, Lucas JM, Murray PD, Thompson SM, Keller A. Zona incerta: a role in central pain. J Neurophysiol. 2009; 102:181–91. [PubMed: 19403748]
37. Quiton RL, M R, Thompson SM, Keller A. Abnormal activity of primary somatosensory cortex in central pain syndrome. J Neurophysiol. 2010; 104:1717–25. [PubMed: 20660417]
38. Seminowicz DA, Jiang L, Ji Y, Xu S, Cullapalli RP, Masri R. Thalamocortical Asynchrony in Conditions of Spinal Cord Injury Pain in Rats. The Journal of Neuroscience. 2012; 32:15843–848. [PubMed: 23136423]
39. Davoody L, Quiton RL, Lucas JM, Ji Y, Keller A, Masri R. Conditioned place preference reveals tonic pain in an animal model of central pain. J Pain. 2011; 12:868–74. [PubMed: 21515090]
40. Cha M, Ji Y, Masri R. Motor cortex stimulation activates the incertothalamic pathway in an animal model of spinal cord injury. J Pain. 2013; 14:260–9. [PubMed: 23332495]
41. Ueki M, Mies G, Hossmann KA. Effect of alpha-chloralose, halothane, pentobarbital and nitrous oxide anesthesia on metabolic coupling in somatosensory cortex of rat. Acta Anaesthesiol Scand. 1992; 36:318–22. [PubMed: 1595336]
42. Gruetter R. Automatic, localized in vivo adjustment of all first- and second-order shim coils. Magn Reson Med. 1993; 29:804–11. [PubMed: 8350724]
43. Sladky R, F K, Tröstl J, Cunnington R, Moser E, Windischberger C. Slice-timing effects and their correction in functional MRI. NeuroImage. 2011; 58:588–94. [PubMed: 21757015]
44. Friston KJ, W S, Howard R, Frackowiak RS, Turner R. Movement-related effects in fMRI time-series. Magn Reson Med. 1996; 35:346–55. [PubMed: 8699946]

NIH-PA Author Manuscript

NIH-PA Author Manuscript

NIH-PA Author Manuscript

45. Poldrack RA. Region of interest analysis for fMRI. Soc Cogn Affect Neurosci. 2007; 2:67–70. [PubMed: 18985121]
46. Cox RW. AFNI: software for analysis and visualization of functional magnetic resonance neuroimages. Comput Biomed Res. 1996; 29:162–73. [PubMed: 8812068]
47. Paxinos, G.; W, C. The rat brain in stereotaxic coordinates. 5th. Burlington, MA: Elsevier Academic Press; 2008.
48. Worsley KJ, Marrett S, Neelin P, Vandal AC, Friston KJ, Evans AC. A unified statistical approach for determining significant signals in images of cerebral activation. Hum Brain Mapp. 1996; 4:58–73. [PubMed: 20408186]
49. Lahti KM, Ferris CF, Li F, Sotak CH, King JA. Imaging brain activity in conscious animals using functional MRI. J Neurosci Methods. 1998; 82:75–83. [PubMed: 10223517]
50. Endo T, Spenger C, Hao J, Tominaga T, Wiesenfeld-Hallin Z, Olson L, et al. Functional MRI of the brain detects neuropathic pain in experimental spinal cord injury. Pain. 2008; 138:292–300. [PubMed: 18258366]
51. Hess A, Sergejeva M, Budinsky L, Zeilhofer HU, Brune K. Imaging of hyperalgesia in rats by functional MRI. Eur J Pain. 2007; 11:109–19. [PubMed: 16517192]
52. Zhao F, Welsh D, Williams M, Coimbra A, Urban MO, Hargreaves R, et al. fMRI of pain processing in the brain: a within-animal comparative study of BOLD vs. CBV and noxious electrical vs. noxious mechanical stimulation in rat. Neuroimage. 2012; 59:1168–79. [PubMed: 21856430]
53. Kanda M, Nagamine T, Ikeda A, Ohara S, Kunieda T, Fujiwara N, et al. Primary somatosensory cortex is actively involved in pain processing in human. Brain Res. 2000; 853:282–9. [PubMed: 10640625]
54. Ohara S, Crone NE, Weiss N, Treede RD, Lenz FA. Cutaneous painful laser stimuli evoke responses recorded directly from primary somatosensory cortex in awake humans. J Neurophysiol. 2004; 91:2734–46. [PubMed: 14602841]
55. Inui K, Wang X, Qiu Y, Nguyen BT, Ojima S, Tamura Y, et al. Pain processing within the primary somatosensory cortex in humans. Eur J Neurosci. 2003; 18:2859–66. [PubMed: 14656335]
56. Vierck CJ, Whitsel BL, Favorov OV, Brown AW, Tommerdahl M. Role of primary somatosensory cortex in the coding of pain. Pain. 2013; 154:334–44. [PubMed: 23245864]
57. Bushnell MC, Duncan GH, Hofbauer RK, Ha B, Chen JI, Carrier B. Pain perception: is there a role for primary somatosensory cortex? Proc Natl Acad Sci U S A. 1999; 96:7705–9. [PubMed: 10393884]
58. Endo T, Spenger C, Westman E, Tominaga T, Olson L. Reorganization of sensory processing below the level of spinal cord injury as revealed by fMRI. Exp Neurol. 2008; 209:155–60. [PubMed: 17988666]
59. Vierck CJ Jr, Greenspan JD, Ritz LA. Long-term changes in purposive and reflexive responses to nociceptive stimulation following anterolateral chordotomy. J Neurosci. 1990; 10:2077–95. [PubMed: 2376769]
60. Peyron R, Faillenot I, Pomares FB, Le Bars D, Garcia-Larrea L, Laurent B. Mechanical allodynia in neuropathic pain. Where are the brain representations located? A positron emission tomography (PET) study. Eur J Pain. 2013
61. Costigan M, Scholz J, Woolf CJ. Neuropathic pain: a maladaptive response of the nervous system to damage. Annu Rev Neurosci. 2009; 32:1–32. [PubMed: 19400724]
62. Canavero, S.; Bonicalzi, V. Central pain sundrome: pathophysiology, diagnosis and management. Cambridge, UK: Cambridge University Press; 2011.
63. Henderson LA, Gustin SM, Macey PM, Wrigley PJ, Siddall PJ. Functional reorganization of the brain in humans following spinal cord injury: evidence for underlying changes in cortical anatomy. J Neurosci. 2011; 31:2630–7. [PubMed: 21325531]
64. Yang Y, Raine A. Prefrontal structural and functional brain imaging findings in antisocial, violent, and psychopathic individuals: a meta-analysis. Psychiatry Res. 2009; 174:81–8. [PubMed: 19833485]

NIH-PA Author Manuscript

NIH-PA Author Manuscript

NIH-PA Author Manuscript

65. Seifert F, Bschorer K, De Col R, Filitz J, Peltz E, Koppert W, et al. Medial prefrontal cortex activity is predictive for hyperalgesia and pharmacological antihyperalgesia. J Neurosci. 2009; 29:6167–75. [PubMed: 19439594]
66. Metz AE, Yau HJ, Centeno MV, Apkarian AV, Martina M. Morphological and functional reorganization of rat medial prefrontal cortex in neuropathic pain. Proc Natl Acad Sci U S A. 2009; 106:2423–8. [PubMed: 19171885]
67. Borsook D, Becerra L. CNS animal fMRI in pain and analgesia. Neurosci Biobehav Rev. 2011; 35:1125–43. [PubMed: 21126534]
68. Bohning DE, Shastri A, Wassermann EM, Ziemann U, Lorberbaum JP, Nahas Z, et al. BOLD-fMRI response to single-pulse transcranial magnetic stimulation (TMS). J Magn Reson Imaging. 2000; 11:569–74. [PubMed: 10862054]
69. Bestmann S, Baudewig J, Siebner HR, Rothwell JC, Frahm J. Functional MRI of the immediate impact of transcranial magnetic stimulation on cortical and subcortical motor circuits. Eur J Neurosci. 2004; 19:1950–62. [PubMed: 15078569]
70. Bestmann S, Baudewig J, Siebner HR, Rothwell JC, Frahm J. BOLD MRI responses to repetitive TMS over human dorsal premotor cortex. Neuroimage. 2005; 28:22–9. [PubMed: 16002305]
71. Rounis E, Lee L, Siebner HR, Rowe JB, Friston KJ, Rothwell JC, et al. Frequency specific changes in regional cerebral blood flow and motor system connectivity following rTMS to the primary motor cortex. Neuroimage. 2005; 26:164–76. [PubMed: 15862216]
72. Peyron R, F I, Mertens P, Laurent B, Garcia-Larrea L. Motor cortex stimulation in neuropathic pain. Correlations between analgesic effect and hemodynamic changes in the brain. A PET study. Neuroimage. 2007; 34:310–21. [PubMed: 17055297]
73. Viisanen H, Pertovaara A. Antinociception by motor cortex stimulation in the neuropathic rat: does the locus coeruleus play a role? Exp Brain Res. 2010; 201:283–96. [PubMed: 19826796]
74. Austin VC, Blamire AM, Grieve SM, O'Neill MJ, Styles P, Matthews PM, et al. Differences in the BOLD fMRI response to direct and indirect cortical stimulation in the rat. Magn Reson Med. 2003; 49:838–47. [PubMed: 12704766]
75. Bogdanova OG, Sil'kis IG. The effects of high-frequency microstimulation of the cortex on interhemisphere synchronization in the rat motor cortex. Neurosci Behav Physiol. 1999; 29:515–22. [PubMed: 10596787]
76. Kobayashi M, Hutchinson S, Schlaug G, Pascual-Leone A. Ipsilateral motor cortex activation on functional magnetic resonance imaging during unilateral hand movements is related to interhemispheric interactions. Neuroimage. 2003; 20:2259–70. [PubMed: 14683727]
77. Innocenti GM, Aggoun-Zouaoui D, Lehmann P. Cellular aspects of callosal connections and their development. Neuropsychologia. 1995; 33:961–87. [PubMed: 8524456]
78. Strafella AP, Paus T. Cerebral blood-flow changes induced by paired-pulse transcranial magnetic stimulation of the primary motor cortex. J Neurophysiol. 2001; 85:2624–9. [PubMed: 11387406]
79. Xu S, Ji Y, Chen X, Yang Y, Gullapalli RP, Masri R. In vivo high-resolution localized (1) H MR spectroscopy in the awake rat brain at 7 T. Magn Reson Med. 2013; 69:937–43. [PubMed: 22570299]
80. Lahti KM, Ferris CF, Li F, Sotak CH, King JA. Comparison of evoked cortical activity in conscious and propofol-anesthetized rats using functional MRI. Magn Reson Med. 1999; 41:412–6. [PubMed: 10080292]
81. Peeters RR, Tindemans I, De Schutter E, Van der Linden A. Comparing BOLD fMRI signal changes in the awake and anesthetized rat during electrical forepaw stimulation. Magn Reson Imaging. 2001; 19:821–6. [PubMed: 11551722]
82. Pagano RL, Fonoff ET, Dale CS, Ballester G, Teixeira MJ, Britto LR. Motor cortex stimulation inhibits thalamic sensory neurons and enhances activity of PAG neurons: Possible pathways for antinociception. Pain. 2012
83. Fonoff ET, Dale CS, Pagano RL, Paccola CC, Ballester G, Teixeira MJ, et al. Antinociception induced by epidural motor cortex stimulation in naive conscious rats is mediated by the opioid system. Behav Brain Res. 2009; 196:63–70. [PubMed: 18718490]

NIH-PA Author Manuscript

NIH-PA Author Manuscript

NIH-PA Author Manuscript

84. Pagano RL, Assis DV, Clara JA, Alves AS, Dale CS, Teixeira MJ, et al. Transdural motor cortex stimulation reverses neuropathic pain in rats: a profile of neuronal activation. Eur J Pain. 2011; 15:268 e1–14. [PubMed: 20817578]
85. Whitt JL, Masri R, Pulimood NS, Keller A. Pathological activity in mediodorsal thalamus of rats with spinal cord injury pain. J Neurosci. 2013; 33:3915–26. [PubMed: 23447602]
86. Power BD, Kolmac CI, Mitrofanis J. Evidence for a large projection from the zona incerta to the dorsal thalamus. J Comp Neurol. 1999; 404:554–65. [PubMed: 9987997]
87. Chang C, Shyu BC. A fMRI study of brain activations during non-noxious and noxious electrical stimulation of the sciatic nerve of rats. Brain Res. 2001; 897:71–81. [PubMed: 11282360]
88. Spornick N, Guptill V, Koziol D, Wesley R, Finkel J, Quezado ZM. Mouse current vocalization threshold measured with a neurospecific nociception assay: the effect of sex, morphine, and isoflurane. J Neurosci Methods. 2011; 201:390–8. [PubMed: 21864576]
89. Koga K, Furue H, Rashid MH, Takaki A, Katafuchi T, Yoshimura M. Selective activation of primary afferent fibers evaluated by sine-wave electrical stimulation. Mol Pain. 2005; 1:13. [PubMed: 15813963]
90. Van Camp N, Verhoye M, Van der Linden A. Stimulation of the rat somatosensory cortex at different frequencies and pulse widths. NMR Biomed. 2006; 19:10–7. [PubMed: 16408324]
91. Bock C, Krep H, Brinker G, Hoehn-Berlage M. Brainmapping of alpha-chloralose anesthetized rats with T2*-weighted imaging: distinction between the representation of the forepaw and hindpaw in the somatosensory cortex. NMR Biomed. 1998; 11:115–9. [PubMed: 9699494]
92. Brinker G, Bock C, Busch E, Krep H, Hossmann KA, Hoehn-Berlage M. Simultaneous recording of evoked potentials and T2*-weighted MR images during somatosensory stimulation of rat. Magn Reson Med. 1999; 41:469–73. [PubMed: 10204868]
93. Burke M, Schwindt W, Ludwig U, Hennig J, Hoehn M. Facilitation of electric forepaw stimulation-induced somatosensory activation in rats by additional acoustic stimulation: an fMRI investigation. Magn Reson Med. 2000; 44:317–21. [PubMed: 10918332]
94. Grune M, Pillekamp F, Schwindt W, Hoehn M. Gradient echo time dependence and quantitative parameter maps for somatosensory activation in rats at 7 T. Magn Reson Med. 1999; 42:118–26. [PubMed: 10398957]
95. Gyngell ML, Bock C, Schmitz B, Hoehn-Berlage M, Hossmann KA. Variation of functional MRI signal in response to frequency of somatosensory stimulation in alpha-chloralose anesthetized rats. Magn Reson Med. 1996; 36:13–5. [PubMed: 8795014]
96. Hyder F, Behar KL, Martin MA, Blamire AM, Shulman RG. Dynamic magnetic resonance imaging of the rat brain during forepaw stimulation. J Cereb Blood Flow Metab. 1994; 14:649–55. [PubMed: 8014212]
97. Tallgren P, Vanhatalo S, Kaila K, Voipio J. Evaluation of commercially available electrodes and gels for recording of slow EEG potentials. Clin Neurophysiol. 2005; 116:799–806. [PubMed: 15792889]
98. Kitzmiller J, Beversdorf D, Hansford D. Fabrication and testing of microelectrodes for small-field cortical surface recordings. Biomed Microdevices. 2006; 8:81–5. [PubMed: 16491335]
99. Jupp B, Williams JP, Tesiram YA, Vosmansky M, O'Brien TJ. MRI compatible electrodes for the induction of amygdala kindling in rats. J Neurosci Methods. 2006; 155:72–6. [PubMed: 16466802]
100. Mirsattari SM, Ives JR, Leung LS, Menon RS. EEG monitoring during functional MRI in animal models. Epilepsia. 2007; 48:37–46. [PubMed: 17767574]

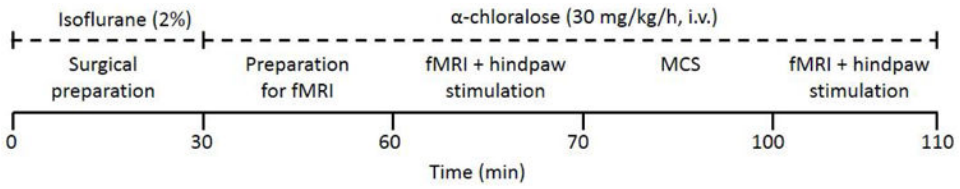

Figure 1.

Functional MRI experimental protocol. Fourteen days after SCL, 2 fMRI sessions were conducted in anesthetized rats undergoing noxious electrical hindpaw stimulation. Motor cortex stimulation was applied for 30 minutes between the two fMRI sessions. Each fMRI session lasted for 10 minutes.

NIH-PA Author Manuscript
NIH-PA Author Manuscript
NIH-PA Author Manuscript

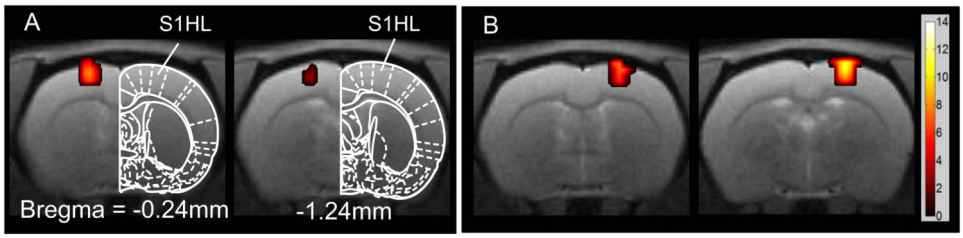

Figure 2.

Brain activation maps in response to electrical stimulation of the hindpaw in naïve animals. (A) Electrical stimulation of the left hindpaw (n=2); (B) Electrical stimulation of right hindpaw in the same animals shown in (A); All activation maps were family wise error-corrected at the cluster level $p < 0.05$ and cluster size is larger than 5 contiguous voxels. All images were superimposed on high resolution T2-weighted image slices (slice thickness = 1 mm) with the reference to the Paxinos and Watson rat brain atlas (47) in terms of distance rostral to or caudal to bregma. All the images here and in the following figures are shown in radiologist convention: left of image = right of brain. The color bar shows the positive statistic T value.

NIH-PA Author Manuscript NIH-PA Author Manuscript NIH-PA Author Manuscript

NIH-PA Author Manuscript

NIH-PA Author Manuscript

NIH-PA Author Manuscript

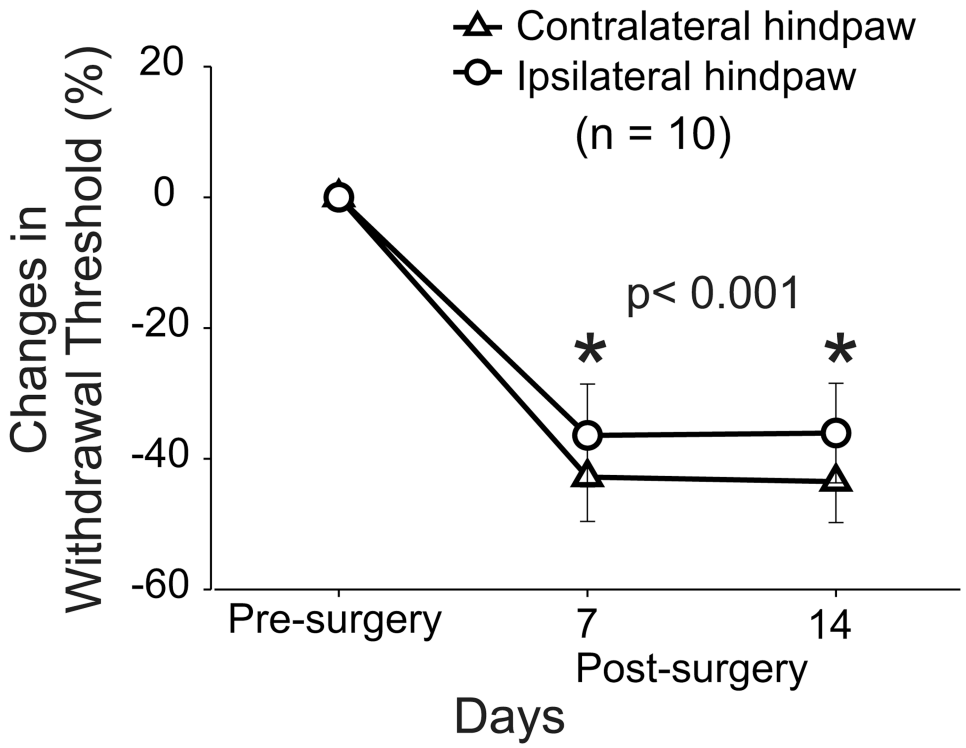

Figure 3.

Behavioral assessment of animals with SCL. Hindpaw (dorsal surface) mechanical withdrawal thresholds decrease bilaterally on days 7 and 14 post-surgery. All values are means ± SE of withdrawal thresholds relative to pre-surgery values. * for statistically significant difference between the pre- and post-surgery withdrawal thresholds for contralateral and ipsilateral hindpaws.

NIH-PA Author Manuscript
NIH-PA Author Manuscript
NIH-PA Author Manuscript

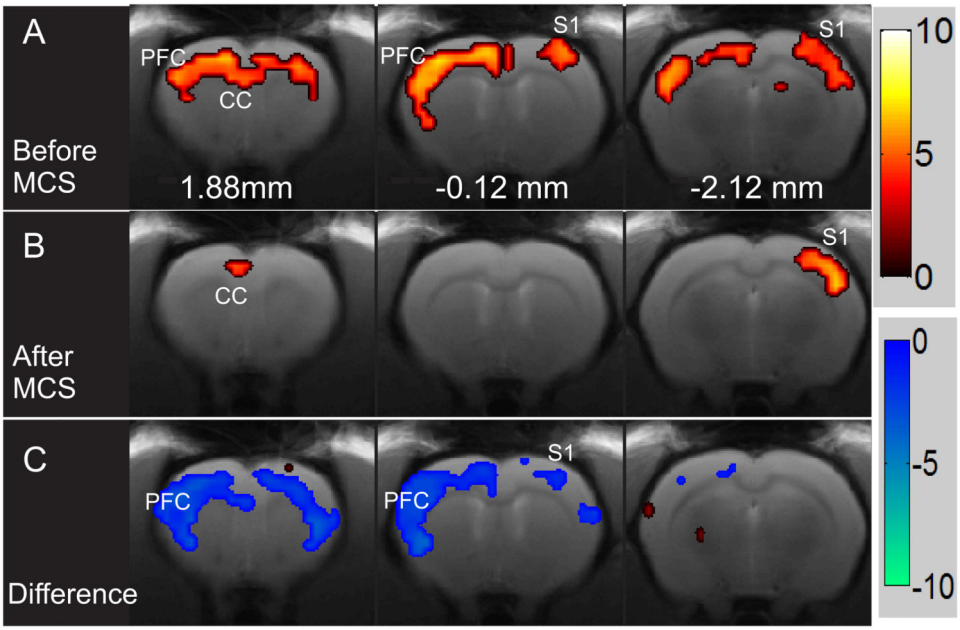

Figure 4.

A representative example of activation maps produced by electrical stimulation of the hindpaw before and after MCS. (A) Activation maps produced by electrical stimulation of the right hindpaw before and after MCS; (B) in the same animal. (C) The difference in activation maps before and after MCS in the same animal presented in A and B. All activation maps were obtained with thresholds of family wise error-corrected $p < 0.05$ and contiguous voxels > 5. Red color bar shows the positive statistic T value. Blue color bar is the negative statistic T value.

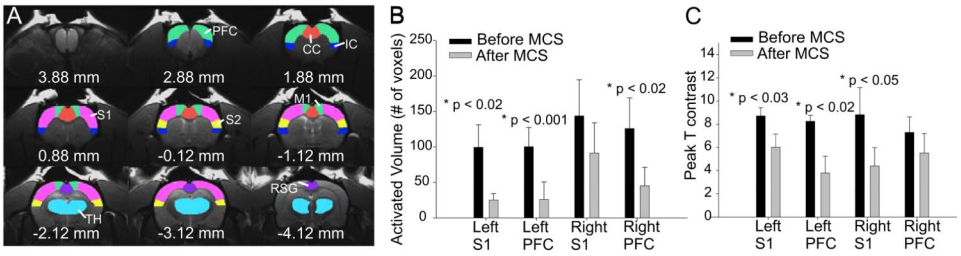

Figure 5.

Region of interest (ROI) selection and summary results in response to electrical stimulation of the right hindpaw. (A) ROI were delineated based on T2-weighted structure images and best approximation to Paxinos and Watson rat brain atlas (47) for each individual rat. Green: prefrontal cortex (PFC); blue: Insular cortex (IC); red: Anterior cingulate cortex (ACC); magenta: primary somatosensory cortex (S1); yellow: second somatosensory cortex (S2); cyan: thalamus (TH). B) The volume of activated voxels changes and (C) peak T value changes in response to electrical stimulation of the right hindpaw before and after MCS. Paired t-test was used to estimate the statistical significance of the extracted measurements of volume.

NIH-PA Author Manuscript
NIH-PA Author Manuscript
NIH-PA Author Manuscript

NIH-PA Author Manuscript
NIH-PA Author Manuscript
NIH-PA Author Manuscript

Table 1

Results of ROI analysis in individual animals.

Animal ID	Left S1			Right S1			Left PFC			Right PFC		
	Cluster *P* (FWE-cor)	Cluster volume	Peak T	Cluster *P* (FWE-cor)	Cluster volume	Peak T	Cluster *P* (FWE-cor)	Cluster volume	Peak *T*	Cluster *P* (FWE-cor)	Cluster volume	Peak *T*
Before MCS												
rat1	0.00E+00	232	9.11	0.00E+00	222	10.74	5.52E−09	207	10.29	1.29E−08	251	10.94
rat2	5.36E−09	99	7.21	1.10E−13	214	7.85	4.32E−09	101	6.55	1.64E−03	196	6.53
rat3	2.80E−07	31	5.89	3.64E−07	30	6.51	8.60E−05	81	6.25	2.89E−04	30	7.08
rat4	7.52E−12	77	10.95				2.34E−04	9	8.90			
rat5	2.18E−04	22	8.49	2.03E−03	10	7.53	3.39E−07	71	8.88	3.11E−04	69	8.47
rat6	2.24E−14	136	11.06	0.00E+00	243	20.55	4.22E−15	133	8.24	0.00E+00	210	8.49
rat7	0.00E+00	333	8.25	0.00E+00	171	8.53	1.11E−16	162	8.65	0.00E+00	190	9.57
After MCS												
rat1	4.91E−07	43	8.61	1.45E−07	50	6.76	3.23E−06	149	9.18	8.35E−05	125	7.94
rat2	6.68E−05	18	5.75				1.93E−02	1	4.75	8.91E−03	5	5.24
rat3												
rat4	3.96E−06	20	5.82									
rat5	1.21E−04	11	5.70	6.23E−09	47	8.60	8.78E−03	6	5.25	1.21E−04	11	6.43
rat6	1.04E−09	60	7.19	0.00E+00	177	8.49				4.59E−09	130	12.58
rat7	0.00E+00	214	9.04	2.78E−14	107	6.97	2.41E−08	140	7.40	9.84E−07	67	6.47